Geochemistry Geophysics Geosystems G3
AN ELECTRONIC JOURNAL OF THE EARTH SCIENCES
Published by AGU and the Geochemical Society

Article
Volume 4, Number 1
2 January 2003
1001, doi:10.1029/2002GC000390
ISSN: 1525-2027

East Asian monsoon forcing of suborbital variability in the Sulu Sea during Marine Isotope Stage 3: Link to Northern Hemisphere climate

Stefanie Dannenmann
Earth and Atmospheric Sciences, University at Albany, State University of New York, Albany, New York, USA

Now at Swiss Federal Institute for Snow and Avalanche Research, Flüelastrasse 11, 7260 Davos Dorf, Switzerland (dannenmann@slf.ch)

Braddock K. Linsley (corresponding author)
Earth and Atmospheric Sciences, University at Albany, State University of New York, 1400 Washington Avenue, Albany, New York, 12222, USA (blinsley@albany.edu)

Delia W. Oppo
Woods Hole Oceanographic Institution, MS#23, Woods Hole, Massachusetts 02543, USA (doppo@whoi.edu)

Yair Rosenthal
Institute of Marine and Coastal Sciences, and Department of Geology, Rutgers, The State University, 71 Dudley Road, New Brunswick, New Jersey 08901, USA (rosentha@imcs.rutgers.edu)

Luc Beaufort
Centre Européen de Recherche et d'Enseignement en Géosciences de l'Environnement (CEREGE), CEREGE-CNRS Europole Mediterranéen de l'Arbois, BP 80 13545, Aix-en-Provence, Cedex 4, France (beaufort@cerege.fr)

[1] We have generated a new high-resolution record of variations in planktonic foraminiferal oxygen isotopes ($\delta^{18}O$) and Mg/Ca from a sediment core (IMAGES 97-2141) in the Sulu Sea located in the Philippine archipelago of western tropical Pacific. This record reveals distinct, suborbital-scale $\delta^{18}O$ changes, most notably during Marine Isotope Stage 3 (MIS3) (~30,000 to 60,000 years B.P.). The amplitudes of these $\delta^{18}O$ fluctuations (0.4 to 0.7‰) exceed that which can be attributed to sea level changes and must be due to changes in sea surface conditions. In the same interval, variations in planktonic foraminifera Mg/Ca suggest that suborbital surface ocean temperature variations of 1 to 1.5°C in the Sulu Sea were not in phase with $\delta^{18}O$. Combined, this evidence indicates that the MIS3 millennial $\delta^{18}O$ events in the Sulu Sea were primarily the result of changes in surface water salinity, which today is directly related to the East Asian Monsoon (EAM) and its influence on the balance between surface water contributions from the South China Sea and Western Pacific Warm Pool (WPWP). Within dating uncertainties the MIS3 Sulu Sea $\delta^{18}O$ suborbital variability indicates that times of fresher surface conditions in the Sulu Sea coincide with similar conditions in the WPWP [*Stott et al.*, 2002] and also with intensifications of the summer EAM as recorded in the U-Th dated Chinese (Hulu Cave) speleothem $\delta^{18}O$ record [*Wang et al.*, 2001] and thus by inference with interstadials in the Greenland Ice core records. Combined, these results indicate that pronounced suborbital variability in the summer EAM and Intertropical Convergence Zone (ITCZ) during MIS3 was tightly coupled with climate conditions in the northern high latitudes.

Components: 6617 words, 4 figures.

Keywords: Paleoceanography; isotope stage 3; SE Asian Monsoon; Mg/Ca; oxygen isotopes; millennial-scale climate change.

Copyright 2003 by the American Geophysical Union

Index Terms: 4267 Oceanography: General: Paleoceanography; 1620 Global Change: Climate dynamics (3309).

Received 11 June 2002; **Revised** 13 August 2002; **Accepted** 29 August 2002; **Published** 2 January 2003.

Dannenmann, S., B. K. Linsley, D. W. Oppo, Y. Rosenthal, and L. Beaufort, East Asian monsoon forcing of suborbital variability in the Sulu Sea during Marine Isotope Stage 3: Link to Northern Hemisphere climate, *Geochem. Geophys. Geosyst.*, *4*(1), 1001, doi:10.1029/2002GC000390, 2003.

1. Introduction

[2] The wealth of data showing suborbital climate variability outside the North Atlantic region has raised important questions about the behavior of tropical climate systems on suborbital scales and their linkage to climate variations in the Northern Hemisphere. Several detailed tropical and subtropical marine and terrestrial archives reveal that low latitude climate systems varied on suborbital timescales at certain times in the late Pleistocene [*Linsley and Thunell*, 1990; *Sirocko et al.*, 1999; *Wang et al.*, 1999; *Peterson et al.*, 2000; *Kienast et al.*, 2001; *Kudrass et al.*, 1991, 2001; *Wang et al.*, 2001; *Stott et al.*, 2002; *Koutavas et al.*, 2002]. However, the number of paleoclimate records from the deep tropics that resolve suborbital climatic variability remains inadequate to temporally and spatially constrain this variability. This is particularly the case for the tropical western Pacific and the important climate components that include the East Asian Monsoon (EAM), the Western Pacific Warm Pool (WPWP) and the Intertropical Convergence Zone (ITCZ).

[3] Important new discoveries pertaining to past changes in the EAM and WPWP come from isotopic results from the midlatitude Hulu Cave (33.5°N) in China [*Wang et al.*, 2001] and from a sediment core off the southeastern coast of the Philippines in the WPWP [*Stott et al.*, 2002]. The Hulu Cave U-Th dated stalagmite $\delta^{18}O$ record strongly suggests that the summer/winter precipitation ratio in the EAM varied on both orbital and suborbital time-scales in the latest Pleistocene and that these variations are synchronous with stadial and interstadial climatic events in the North Atlantic. Specifically, times of summer monsoon dominance correlate to North Atlantic interstadials. The *Stott et al.* [2002] results indicate lower salinity conditions in the WPWP during interstadials of Marine Isotope Stage 3 (MIS3) in conjunction with intensification of the ITCZ. In this contribution we present new evidence from a sediment core recovered from the Sulu Sea at 8.8°N in the western tropical Pacific indicating that both surface salinity and temperature varied on 5–10 Kyr timescales (''Dansgaard/Oeschger''; D/O) during MIS3. Whereas salinity variations appear to be driven by variations in the EAM, the Sulu Sea surface temperature record appears to co-vary with the Antarctic Byrd $\delta^{18}O$ record suggesting that temperature in this region may share a common forcing with Antarctic air temperature. Thus, suborbital variations in surface ocean properties at this single tropical site exhibit the fingerprint of both northern Hemisphere and southern Hemisphere high latitude climate.

2. Hydrography

[4] The Sulu Sea is a marginal basin in the western tropical Pacific with a maximum depth of more than 4900 m. The basin exchanges surface water with surrounding basins over shallow sills, with the deepest sill connecting the Sulu Sea to the South China Sea at 420 m through the Mindoro Strait [*Wyrtki*, 1961]. The South China and Sulu Seas are located in the northern part of the Asian-Australian monsoon region where increased precipitation during the summer months is the result of the increased influence of the ITCZ as part of the EAM. The high average annual atmospheric temperatures in the region induce evaporation of oceanic water, formation of low-pressure cells and seasonally heavy rain. During the Northern Hemisphere summer monsoon, winds blow from the southeast and bring the seasonal precipitation

maximum. The winter component of the EAM has a stronger northwesterly wind field, with less associated precipitation [*Chen et al.*, 1997].

[5] Seasonal sea surface temperature (SST) variability is greater in the northern South China Sea than the Sulu Sea due to the inflow of cold water through the Luzon Strait and excess evaporation that reduces SSTs during the months of the winter monsoon (Figure 1). Annually, SST varies about 2°C in the Sulu Sea and southern South China Sea (Figure 1) compared to 5°C in the northern South China Sea. Salinity in the entire region varies seasonally between 32.8 and 34.5‰. In the Sulu Sea, seasonal variations in monsoon precipitation, riverine discharge, and in the direction of surface currents result in a 0.5‰ annual surface salinity variation with a surface salinity minimum occurring on average in October [*Wyrtki*, 1961; *Conkright et al.*, 1998] (Figure 1). The high average annual precipitation leads to an overall hydrologic balance where there is a gain of fresh water from precipitation.

[6] On interannual time-scales, the El Niño Southern Oscillation (ENSO) affects the Sulu Sea and South China Sea in significantly different ways. Climatic conditions in the southern South China Sea are more strongly correlated to ENSO whereas the Sulu Sea is located at a correlation "hinge" point with a weaker correlation to ENSO. The center of convection and precipitation moves eastward into the central Pacific, away from the Sulu Sea and WPWP during El Niño events [*Waliser and Gautier*, 1993; *Hoerling et al.*, 1997]. These are times when rainfall totals associated with the Indian summer monsoon, the East Asian summer monsoon, and the North Australian summer monsoon, are all generally well below average [*Webster et al.*, 1998]. Under La Niña conditions, strong trade winds fuel a more intense summer monsoon, and areas of eastern China, Thailand, and the South China Sea experience increased precipitation. Also, during La Niña events, rainfall increases slightly in the Sulu Sea, and increases dramatically to the west in the core of the WPWP. On interannual timescales SST in both basins varies in response to the phase of ENSO. During El Niño events, SST in the Sulu Sea decreases slightly, contrasting with a strong warming in the southern South China Sea that lags several months behind the peak of El Niño events [*Klein et al.*, 1999].

[7] During the Holocene and latest Pleistocene, long-term changes in monsoon and/or ENSO driven sea surface salinity (SSS) and circulation in the South China Sea should have directly influenced SSS of the Sulu Sea. Changes in sea level could also have served to amplify the effect of the South China Sea on the Sulu Sea. Due to the relatively lower sea level during MIS3, the Sunda Shelf route of surface water circulation into the Indian Ocean was at least partially blocked and it is possible that more of the fresh water discharge from rivers draining South East Asia was focused in the Sulu Sea region. The lower sea level at this time could have also amplified the influence of rivers draining Borneo and the Philippines.

3. Methodology

[8] Here we discuss temporal $\delta^{18}O$ and Mg/Ca variations in the planktonic foraminifera *Globigerinoides ruber* from Sulu Sea IMAGES core MD97-2141 (8.8°N, 121.3°1 E, 3,633 m water depth) during MIS3. The core was collected within several kilometers of ODP site 769A to expand on earlier results from Site 769 [*Linsley and Thunell*, 1990; *Linsley and Dunbar*, 1994; *Linsley*, 1996]. The entire core was slab-sampled and analyzed at 1 cm resolution for $\delta^{18}O$ giving this new record four times greater temporal resolution (<100 years) than the previously published $\delta^{18}O$ record for *G. ruber* ($\delta^{18}O_{G.\ ruber}$) from ODP site 769A [*Linsley*, 1996]. Each sample for isotopic analysis consisted of ~10 individual tests (~100 μg) of *G. ruber* (white variety; 212–250 μm in diameter). Samples were reacted with 100% H_3PO_4 at 90°C in a MultiPrep carbonate preparation device. The resulting CO_2 gas was analyzed with a Micromass Optima dual-inlet mass spectrometer at the University at Albany, State University of New York. The standard deviation of the National Institute of Science and Technology international reference standard (NBS-19) analyzed over an 8 month time period (n = 498) was 0.036‰ for $\delta^{18}O$. All isotopic data are reported relative to the Vienna Peedee Belemnite

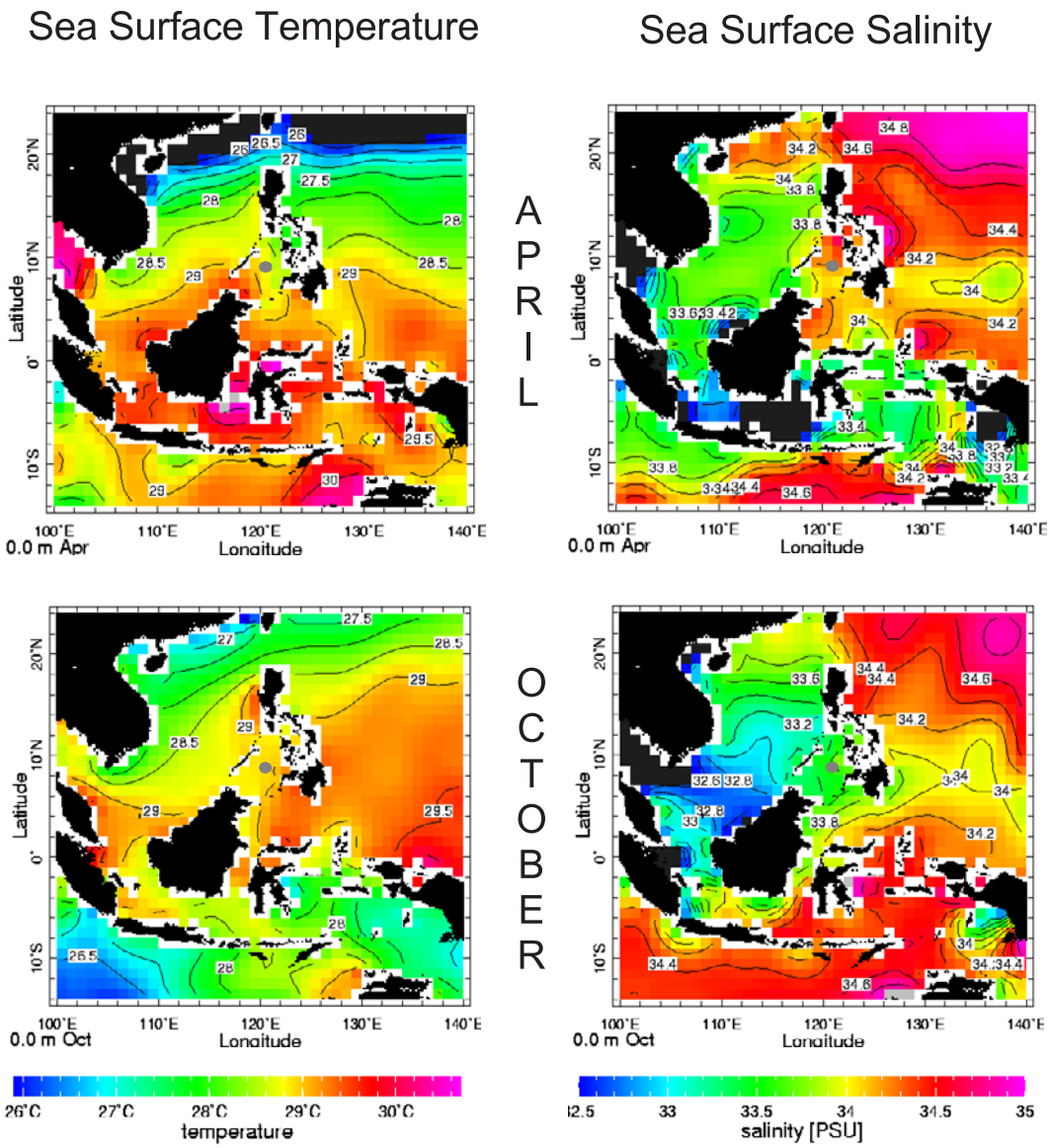

Figure 1. Average sea surface temperature and sea surface salinity in Indonesia and the western Pacific for the end of the Northwest winter monsoon (April) and end of the Southeast summer monsoon (October), highlighting maximum seasonal monsoon changes in surface conditions. Note the location of IMAGES core MD97-2141 that is marked by a gray circle. In the Sulu Sea the influence of East Asian Monsoon-driven river runoff and precipitation in Borneo and coastal regions of the mainland is evident as is the influence of the western Pacific on surface salinity (data from *Conkright et al.* [1998]).

(VPDB) using the standard δ notation. The average difference in $\delta^{18}O$ between duplicate analyses of the same sample of *G. ruber* (n = 283) was 0.094‰ [*Dannenmann*, 2001].

[9] Mg/Ca of *G. ruber* was measured in samples at approximately 2 cm intervals in MIS3. The cleaning procedure for the Mg/Ca analyses followed the protocol of *Rosenthal et al.* [1999]. Approximately 80 shells of *G. ruber* (212–300 μm sieve-size fraction) were picked and weighed with a Mettler M3 microbalance (nominal precision ±1 μg). After weighing, each sample was gently crushed to open the chambers. The crushed samples were washed with deionized water, ultrasonicated and rinsed with methanol. The rinsed samples were treated with a

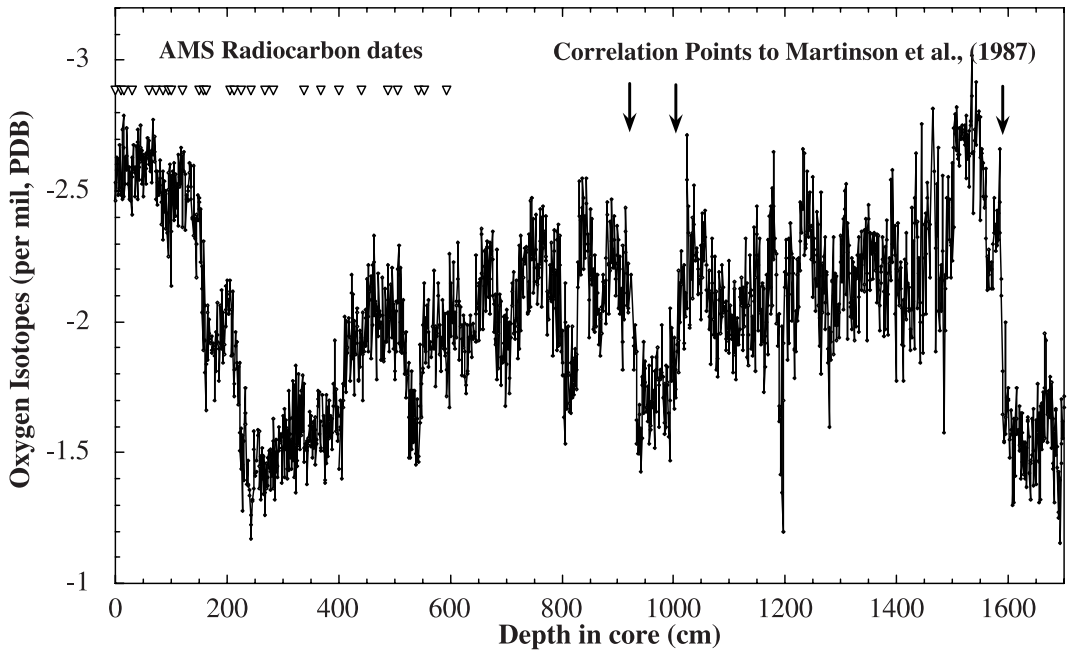

Figure 2. Sulu Sea $\delta^{18}O$ record of *G. ruber* ($\delta^{18}O_{G.\ ruber}$) versus depth in IMAGES core MD97-2141. Triangles denote depths of AMS radiocarbon dates (see text) and arrows denote location of three correlation points to the *Martinson et al.* [1997] chronology.

hot basic oxidizing solution followed by multiple weak acid leaching (0.002 HNO_3). The cleaned samples were dissolved with HNO_3. Several authors [*Brown and Elderfield*, 1996; *Hastings et al.*, 1998] concluded that this cleaning procedure is sufficient for Mg/Ca analysis in foraminifera. Mg/Ca ratios were determined using a Finnigan MAT Element Sector Field ICP-MS at Rutgers University following methods discussed in *Rosenthal et al.* [1999]. The external precision of the Mg/Ca ratio was ±1.2% as determined by repeated measurements of three consistency standards. The average standard error (1σ) for replicate samples was ±0.30 μg for weight measurements and ±0.12 mmol mol^{-1} for Mg/Ca analyses, resulting in a ±0.60°C pooled error of the temperature estimate.

[10] The age model for the upper 17 m of core MD97-2141 consists of 28 accelerator mass spectrometry (AMS) radiocarbon age dates (open triangles in Figure 2; *de Garidel-Thoron et al.* [2001] and *Dannenmann* [2001]), and 3 correlation points to the *Martinson et al.* [1987] chronology (arrows in Figure 2). The AMS-dates at the sample depths 400 cm and 421 cm indicate a gap of 11,000 years and identify the presence of an erosional hiatus. A hiatus has not been observed in adjacent ODP769A site [*Linsley*, 1996], but this might be due to the lower resolution AMS ^{14}C dating of this core.

4. Results

[11] The MD97-2141 *G. ruber* $\delta^{18}O$ record exhibits significant suborbital variability and confirms the presence of abrupt climatic events in the Sulu Sea during the Younger Dryas Chronozone and during MIS 5e (Figures 2 and 3b) [*Linsley and Thunell*, 1990; *Kudrass et al.*, 1991; *Linsley*, 1996]. In addition, previously unrecognized millennial-scale $\delta^{18}O$ changes in *G. ruber* are clearly seen in the Sulu Sea during MIS3. The amplitude of these oscillations, ranging from 0.4 to 0.7‰, is approximately half of the glacial-interglacial $\delta^{18}O$ amplitude observed at this site. In the same interval, planktonic foraminiferal Mg/Ca exhibits suborbital variability on the order of 0.5 mmol mol^{-1} (Figures 3d and 3f).

[12] Estimating SST from the Mg/Ca data is not straightforward. Currently available calibrations of Mg/Ca versus temperature that were used for reconstructing SST in other Pacific cores [*Lea et*

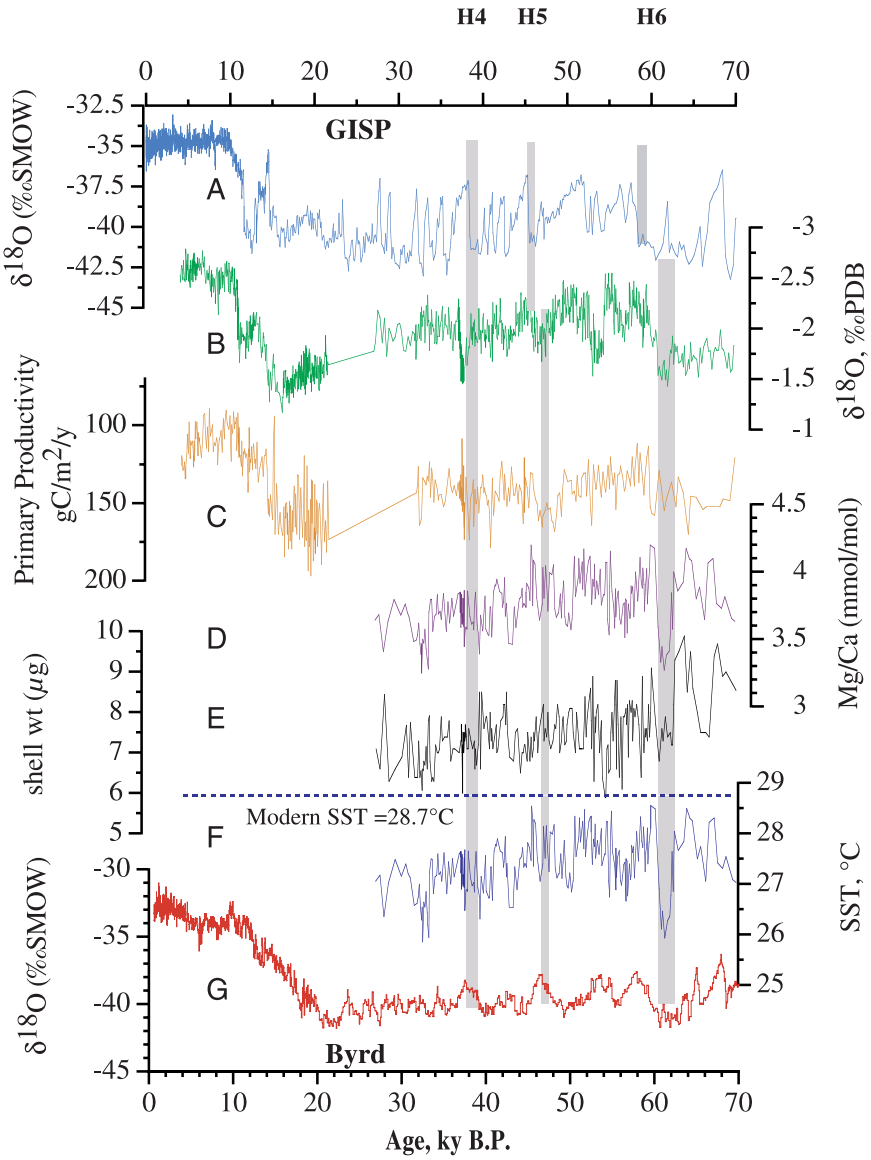

Figure 3. Data from the Sulu Sea during the last 70 Kyr compared to Greenland ice core $\delta^{18}O$. (a) Greenland Ice core (GISP2) $\delta^{18}O$ data [*Blunier and Brook*, 2001]. Occurrences of Heinrich events H4, H5, and H6 are indicated. (b) Sulu Sea $\delta^{18}O_{G.\ ruber}$. (c) Sulu Sea primary productivity as reconstructed from the coccolithophorid record [*de Garidel-Thoron et al.*, 2001]. (d) Sulu Sea $Mg/Ca_{G.\ ruber}$. (e) Average *G. ruber* shell mass in μg. Arrow marks the core-top shell weight. (f) Mg/Ca-based SST estimates. (g) Byrd ice core $\delta^{18}O$ data [*Blunier and Brook*, 2001].

al., 2000; *Dekens et al.*, 2002] cannot be applied to the Sulu Sea record. Carbonate preservation in the Sulu Sea is generally much better than in the open Pacific Ocean [*Linsley et al.*, 1985; *Miao et al.*, 1994] because the basin is filled with subsurface waters entering through the shallow sills and because the residence time of these waters within the Sulu Sea is relatively short [*Nozaki et al.*, 1999]. The high $CaCO_3$ preservation results in relatively high planktonic foraminiferal Mg/Ca [*Rosenthal et al.*, 2000]. If the open-ocean calibration for converting Mg/Ca to SST is used [*Lea et al.*, 2000], SST estimates are unreasonably high. This is because the calibration was performed with core tops having undergone some post-depositional dissolution and Mg loss. Hence, we use a new dissolution-corrected calibration for *G. ruber* [*Rosenthal and Lohmann*, 2002]. This calibration is based on the observation of a strong linear correlation between changes in foraminiferal test

weight/size ratio and bulk foraminiferal test Mg/Ca in core-top samples and the degree of calcite saturation of the bottom water. In the new calibration the pre-exponential constant is linearly correlated with the extent of preservation/dissolution of the foraminiferal shell, expressed as a function of the size-normalized shell weight (wt.): $(Mg/Ca)_{G.\ ruber} = (0.025wt + 0.11)Exp(0.095SST)$ [*Rosenthal and Lohmann*, 2002], and hence minimizes the influence of dissolution, which is known to preferentially lower foraminiferal Mg/Ca [*Brown and Elderfield*, 1996; *Rosenthal et al.*, 2000]. Using the average, core-top shell weight (212–300 μm size fraction) of 6.74 μg, the Mg-temperature relationship for the Sulu Sea is $(Mg/Ca)_{G.\ ruber} = 0.279Exp(0.095SST)$. Applying this equation to core top Mg/Ca of 4.32 mmol mol^{-1} we estimate SST of 28.9°C, in excellent agreement with modern mean annual value of 28.7°C [*Levitus and Boyer*, 1994]. We use the latter equation (i.e., assuming a constant shell weight of 6.74 μg) for the entire record of MIS3.

[13] Several lines of evidence argue against a significant dissolution influence on the Mg/Ca record during MIS3. Today, the Sulu Sea calcite lysocline and aragonite compensation depth occur near 3800 m and 1400 m, respectively, significantly deeper than in the adjacent open Pacific and South China Sea [*Linsley et al.*, 1985; *Miao et al.*, 1994]. The high carbonate saturation level is related to the chemistry and temperature of the water entering the basin through the shallow sills separating the Sulu Sea from the Pacific Ocean and South China Sea. Past studies indicate enhanced carbonate preservation in the Sulu Sea during the last glaciation [*Linsley and Thunell*, 1990; *Miao et al.*, 1994] and upper section of MIS3 relative to the Holocene. This is likely related to the fact that with sea level lowering, the water entering the deep Sulu Sea originates closer to the surface and has a higher carbonate ion concentration. In the Sulu Sea, planktonic foraminiferal Mg/Ca decreases from 4 mmol mol^{-1} at 60 ka B.P. to 3.55 mmol mol^{-1} at 30 ka B.P. During this interval the average shell weight is 7.2 ± 0.5 μg and is not significantly different than that of core-top samples (Figure 3e). This suggests that carbonate preservation was similar or slightly better than at present. Therefore, we believe that variations in foraminiferal Mg/Ca observed during MIS3 are primarily driven by temperature rather than dissolution.

[14] During MIS3, our Mg/Ca-based SST estimates suggest that on average, Sulu Sea SST was about 2°C colder throughout MIS3 than at present and there appears to be a small cooling trend of ~0.5°C from early to late MIS3 (Figure 3f). This estimate is comparable with the Mg/Ca, and U^{K}_{37} -based estimates of ~2°C cooling during MIS3 from the Ontong Java Plateau (OJP) [*Lea et al.*, 2000] and southern SCS [*Pelejero et al.*, 1999]. The Mg/Ca record also indicates the occurrence of millennial-scale variability in Sulu Sea SST on the order of 1 to 1.5°C.

[15] We calculated $\delta^{18}O_{seawater}$ for the interval from 70 to 28 Kyr by removing the SST-driven component of changes in *G. ruber* $\delta^{18}O$ using the relationship 1°C = −0.22‰ [*Bemis et al.*, 1998] (Figure 4d). Throughout MIS3, $\delta^{18}O_{seawater}$ in the Sulu Sea remains ~0.4‰ lower than $\delta^{18}O_{seawater}$ in the WPWP [*Lea et al.*, 2000; *Stott et al.*, 2002]. This is apparently due to the effects of lower sea level, a generally weaker summer monsoon, and a stronger winter monsoon, all favoring the input of lower salinity South China Sea surface water to the Sulu Sea over saltier WPWP surface water at this time [*Oppo et al.*, 2002].

[16] The $\delta^{18}O_{seawater}$ record clearly shows several ~0.5‰ suborbital variations within MIS3 and MIS4 that generally coincide with the lower resolution WPWP $\delta^{18}O_{seawater}$ record calculated here using the *Stott et al.* [2002] $\delta^{18}O_{G.\ ruber}$ and *G. ruber* Mg/Ca-based SST results and the *Bemis et al.* [1998] equation (Figure 4d). Comparison to coral-based sea level estimates [*Chappell et al.*, 1996; *Yokoyama et al.*, 2001] converted to $\delta^{18}O$ (Figure 4d) [125m = 1‰; *Chappell*, 2002] suggests that approximately 0.1 to 0.2‰ of the 0.5‰ MIS3 $\delta^{18}O_{seawater}$ variations may be due to suborbital changes in sea level [*Yokoyama et al.*, 2001]. The remaining ~0.3‰ additional $\delta^{18}O$ change in the MIS3 $\delta^{18}O$ events is most likely due to changes in sea surface salinity (SSS). In addition, the presence of the 8.2 kyr event in Sulu Sea $\delta^{18}O$ (a time of

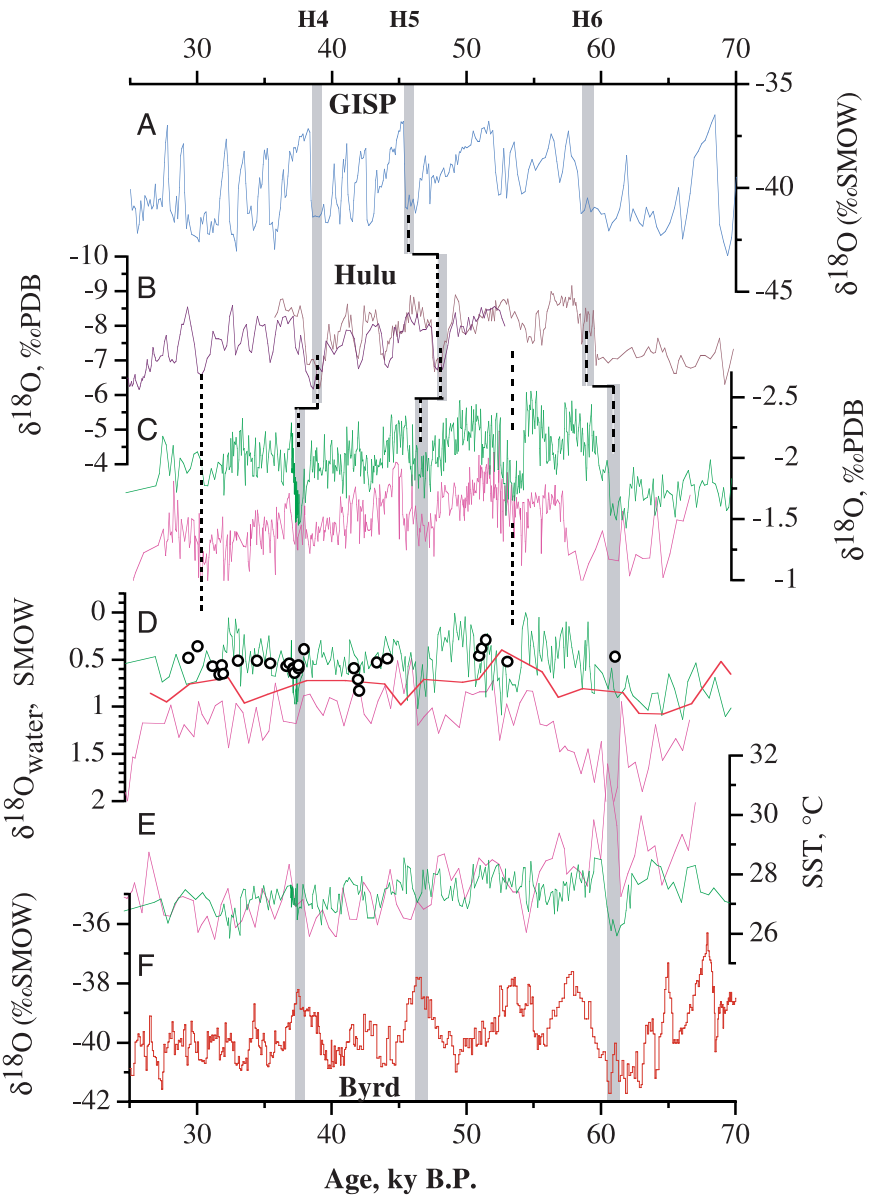

Figure 4. Comparison of the isotopic records from Greenland and Antarctica to isotopic and trace element data from the Sulu Sea and Mindanao and isotopic data from the Chinese Hulu Cave between 25 and 70 Kyr. The Greenland and Antarctica timescales are based on correlating atmospheric methane records from these cores [*Blunier and Brook*, 2001]. Sulu Sea data are on an independent timescale. (a) Greenland Ice core (GISP2) $\delta^{18}O$ data [*Blunier and Brook*, 2001]. Occurrences of Heinrich events H4, H5, and H6 are indicated. (b) $\delta^{18}O$ of Hulu Cave stalagmites in China [*Wang et al.*, 2001]. (c) Sulu Sea $\delta^{18}O_{G.\ ruber}$ of MD97-2141 (green) compared with the WPWP record of MD97-2181 (purple; *Stott et al.* [2002]) (d) Sulu Sea $\delta^{18}O_{seawater}$ (green) has been calculated using the empirically derived temperature-$\delta^{18}O$ relationship based on planktonic foraminifera generated by *Bemis et al.* [1998] and Mg/Ca - derived SST. Superimposed are sea level data (black open circles) reported by *Chappell et al.* [1996] and *Yokoyama et al.* [2001]. Red curve is $\delta^{18}O_{seawater}$ for the central WPWP from *Lea et al.* [2000] and purple curve is $\delta^{18}O_{seawater}$ for the WPWP calculated using the *Stott et al.* [2002] results and the same method we used with the Sulu Sea data presented here. (e) Mg/Ca temperature estimates for the Sulu Sea (green) and WPWP (purple; *Stott et al.* [2002]). (f) Byrd ice core $\delta^{18}O$ data [*Blunier and Brook*, 2001].

minimal sea level change) and the Younger Dryas oscillation (not associated with a large global sea level event [*Fairbanks*, 1989]) also argue against complete sea level control of suborbital $\delta^{18}O_{seawater}$ variability in the Sulu Sea (Y. Rosenthal et al., The amplitude and phasing of climate change during the last deglaciation in the Sulu Sea, western equatorial Pacific, manuscript in preparation, 2002) (Figure 3). Assuming that ~0.3‰ of the $\delta^{18}O_{seawater}$ events was due only to SSS variations, these scale to approximately 0.6 p.s.u. [*Broecker and Denton*, 1989] to 1.0 p.s.u. [*Fairbanks et al.*, 1997] salinity variations. Based on current hydrography, the most probable cause of the $\delta^{18}O_{seawater}$ variations during MIS3 is past variability of the ITCZ/EAM system, both due to its influence on precipitation and on the surface flows that control the relative input of fresh SCS versus saltier WPWP waters.

5. Discussion

[17] The connection between European climate and the Asian monsoons has been the focus of many recent observational and modeling studies. These studies suggest that heavy snow cover over Eurasia in winter is usually followed by a weak summer monsoon, largely because delayed snowmelt results in cooler spring and summer temperatures and reduces the land-sea temperature contrast [*Barnett et al.*, 1989; *Douville and Royer*, 1996, and references therein]. *Overpeck et al.* [1996] extended these results to the Younger Dryas cold event by showing that cold North Atlantic SSTs and a moderate-sized Scandinavian ice sheet resulted in a delay of Tibetan Plateau snowmelt in a model. While focusing on the Younger Dryas, suborbital variations in North Atlantic SSTs would possibly have a similar influence on the land-sea temperature contrasts, and hence monsoon intensity, during MIS3.

[18] Previous studies of sediment cores from the northern South China Sea found millennial-scale changes in precipitation and runoff that were thought to be related to the East Asian monsoon system [*Wang et al.*, 1999]. Additional strong evidence for suborbital EAM variability comes from speleothems in the Hulu Cave in China (33.5°N; 119°E). The Hulu Cave stalagmites have yielded a reproduced U-Th dated $\delta^{18}O$ record of interpreted EAM variability [*Wang et al.*, 2001] spanning 11,000 to 75,000 years B.P. (Figure 4b). This record exhibits pronounced suborbital variations that are remarkably similar to those observed in the Greenland ice cores during MIS3 with times of summer monsoon dominance correlating to North Atlantic interstadials. The strong similarity between the timing and relative amplitude of changes in the Hulu Cave $\delta^{18}O$ and Sulu Sea $\delta^{18}O_{seawater}$ records indicates that suborbital variations in the summer EAM exerted a profound influence on the surface hydrography of the SCS and Sulu Sea. Apparent temporal offsets between the two records are probably due to errors in the less constrained Sulu Sea MIS3 chronology.

[19] In the Sulu Sea, coccolithophore-based primary productivity (PP) estimates from the same core analyzed in this study, have been proposed as an index of Northwest winter EAM variability [*de Garidel-Thoron et al.*, 2001] (Figure 3c). A high PP index records times of a shallower nutricline due to increased wind stress under an intensified winter monsoon [*de Garidel-Thoron et al.*, 2001]. This PP index of EAM variability also shows a weak correlation to North Atlantic climate variability (Figure 3). However, the stronger resemblance of the Sulu Sea $\delta^{18}O_{seawater}$ record suggests tighter coupling between Sulu Sea region precipitation/runoff/surface flow and the EAM/North Atlantic than between the changes in PP and higher latitude climate variability (Figure 4). The reason for this difference in Sulu Sea monsoon proxies is unclear, but may indicate additional, complicating influences on primary productivity, or a nonlinear response of PP to EAM forcing.

[20] The U-Th dated Hulu Cave $\delta^{18}O$ record indicates that variability of the southeast EAM (Figure 4) is closely tied to changes in Greenland air temperatures with times of summer monsoon dominance correlating to North Atlantic interstadials [*Wang et al.*, 2001]. The EAM provides a link between North Atlantic climate and the Sulu Sea. During MIS3, relatively fresh surface waters in the

Sulu Sea coincide with a greater summer/winter precipitation ratio in the EAM, and also with the warm phases of suborbital cycles in the North Atlantic. This result suggests that suborbital climate variability during MIS3 in the Northern Hemisphere and in the low latitudes maybe connected via the WPWP (and Indian Ocean) to the North Atlantic. Using modern instrumental SST data, a similar conclusion was reached by *Hoerling et al.* [2001], who found that the recent 20th century warming of the tropical western Pacific and Indian Oceans has forced a commensurate trend in the North Atlantic.

[21] Unlike $\delta^{18}O$, the Sulu Sea Mg/Ca-based SST record shows little resemblance to high latitude Northern Hemisphere climatic change. Throughout MIS3, Mg/Ca-based SST estimates suggest that on average, Sulu Sea SST was about 2°C colder than present (see Figure 3f). The Mg/Ca record also indicates the occurrence of suborbital variability in Sulu Sea SST throughout MIS3 on the order of 1 to 1.5°C (Figures 3 and 4). The sign and timing of this variability appears closely related to variability in the Antarctic Byrd ice core $\delta^{18}O$ (Figure 4). Understanding the nature of the possible linkage between Antarctic air temperatures and the Sulu Sea Mg/Ca-SST record is difficult. One potential explanation involves long-term changes in the ENSO system, perhaps coupled to changes in the EAM.

[22] Modeling experiments suggest that ENSO could vary on millennial time-scales [*Clement et al.*, 1999], and perhaps drive millennial variability elsewhere [*Schmittner and Clement*, 2002]. Under this scenario an interval of more numerous El Niño-warm mode events would favor the melting of Northern Hemisphere ice sheets [*Cane*, 1998; *Clement and Cane*, 1999]. The recent modeling results of *Schmittner and Clement* [2002] support climatological evidence [*Weyl*, 1968; *Latif et al.*, 2000; *Latif*, 2001] suggesting that times of more frequent or prolonged El Niño warm phase events result in a net transport of fresh water from the Atlantic to the Pacific, thus making the surface of the tropical Atlantic saltier. This in-turn enhances thermohaline circulation in the Atlantic and slightly warms the North Atlantic [*Schmittner and Clement*, 2002]. The opposite is true at the Antarctic Peninsula where El Niño-warm events tend to be times of extensive sea ice [*Yuan and Martinson*, 2000]. Thus suborbital ENSO teleconnections could drive changes of opposite sign in both the high latitude Northern and Southern Hemispheres which is a possible explanation for the apparent northern Hemisphere response of the Sulu Sea $\delta^{18}O_{seawater}$ signal and the Southern Hemisphere response of the Sulu Sea Mg/Ca signal during MIS3.

[23] Possible paleoceanographic evidence for suborbital ENSO variations has recently come from the far western tropical Pacific. Using a sediment core from the open WPWP near the Philippines, *Stott et al.* [2002] have documented suborbital variations in MIS3 $\delta^{18}O_{seawater}$ that also indicate higher (lower) salinities during stadials (interstadials). They suggest that these suborbital $\delta^{18}O_{seawater}$ variations in MIS3 resulted from variations in the ITCZ and timing of the EAM. They further suggest that these suborbital salinity variations in the WPWP are consistent with a long-term (suborbital) ENSO hypothesis with El Niño-like conditions correlating with stadials in high latitudes and La Niña conditions correlating with interstadials.

[24] As previously discussed, the current climatic response of the Sulu Sea to ENSO forcing is complex due to its location on a correlation hinge point between the EAM and WPWP. For example, while the WPWP warms and receives more rainfall during La Niña events, the southern South China Sea cools and receives less rainfall. During ENSO events under present boundary conditions, the Sulu Sea appears to register a mixed SST and precipitation response from both the South China Sea and the WPWP. Thus, although our results cannot be used to directly support an ENSO mechanism for late Pleistocene suborbital climatic variability, they are consistent with such a mechanism. Evidence in the Cariaco Basin for enhanced precipitation and runoff during MIS3 interstadials [*Peterson et al.*, 2000] is also consistent with this mechanism [*Stott et al.*, 2002; *Oppo et al.*, 2002]. We add however, that remote ENSO teleconnections like those to the North Atlantic or Antarctica

may differ under different boundary conditions, and hence additional highly resolved records to test an ENSO mechanism should come from tropical areas dominated by ENSO variability today, rather than from remote or correlation hinge-point regions like the Sulu Sea that only exhibit ENSO-related climate variability. Furthermore, as discussed in a companion paper [*Oppo et al.*, 2002], modeling studies suggest ways that tropical regions respond to known suborbital changes in the North Atlantic region, and hence even the direction of tropical-extratropical connections on suborbital timescales continues to be a subject of lively debate.

[25] In summary, our data unambiguously demonstrate that the effect of suborbital variations in the summer EAM extended beyond the South China Sea, into the Sulu Sea, and also coincide with suborbital surface ocean variability in the WPWP [*Stott et al.*, 2002]. Our results, showing that the Sulu Sea records the fingerprint of both Northern and Southern Hemisphere climate change, is consistent with variability of ENSO on suborbital cycles, and underscores the need for more records that unambiguously record long-term changes in ENSO variability.

Acknowledgments

[26] We thank the IMAGES Program for allowing access to core MD97-2141, S. Howe for help with stable isotopes analyses, S. Trimarchi for help with AMS sample preparation. The AMS-data were generated at the WHOI-NOSAMS AMS facility. We greatly appreciate comments from M. A. Cane and R. C. Thunell. This project has been funded by NSF Awards OCE 9710156 to BKL and, OCE 9710097 to DWO, and OCE 9987060 to YR. We also acknowledge the support of French MENRT, TAAF, CNRS/INSU and IFRTP to the Marion Dufresne and the IMAGES program. This is WHOI contribution number 10693.

References

Barnett, T. P., L. Dumenil, U. Schlese, E. Roeckner, and M. Latif, The effect of Eurasian snow cover on regional and global climate variations, *J. Atmos. Sci.*, *46*, 661–685, 1989.

Bemis, B. E., et al., Reevaluation of the oxygen isotopic composition of planktonic foraminifera: Experimental results and revised paleotemperature equations, *Paleoceanography*, *13*, 150–160, 1998.

Blunier, T., and E. J. Brook, Timing of millennial-scale climate change in Antarctica and Greenland during the last glacial period, *Science*, *291*, 109–112, 2001.

Broecker, W. S., and G. H. Denton, The role of ocean-atmosphere reorganizations in glacial cycles, *Geochim. Cosmochim. Acta*, *53*, 2465–2501, 1989.

Brown, S. J., and H. Elderfield, Variations in Mg/Ca and Sr/Ca ratios of planktonic foraminifera caused by post-depositional dissolution: Evidence of shallow Mg-dependent dissolution, *Paleoceanography*, *11*, 543–551, 1996.

Cane, M. A., A role for the tropical Pacific, *Science*, *282*, 59–61, 1998.

Chappell, J., Sea Level changes forced ice breakouts in the Last Glacial cycle: New results from coral terraces, *Quat. Sci. Rev.*, *21*, 1229–1240, 2002.

Chappell, J., A. Omura, T. Esat, M. McCulloch, J. Pandolfi, Y. Ota, and B. Pillans, Reconciliation of late Quaternary sea levels derived from coral terraces at Huon Peninsula with deep sea oxygen isotope records, *Earth Planet. Sci. Lett.*, *141*, 227–236, 1996.

Chen, F. H., J. Bloemendal, J. M. Wang, J. J. Li, and F. Oldfield, High-resolution multi-proxy climate records from Chinese loess: Evidence for rapid climatic changes over the last 75 kyr, *Palaeogeogr. Palaeoclimatol. Palaeoecol*, *130*, 323–335, 1997.

Clement, A. C., R. Seager, and M. A. Cane, Orbital controls on the El Niño/Southern Oscillation and the tropical climate, *Paleoceanography*, *14*, 441–456, 1999.

Conkright, M., S. Levitus, T. O'Brien, T. Boyer, J. Antonov, and C. Stephens, World Ocean Atlas 1998 CD-ROM Data Set Documentation, *Tech. Rep. 15*, 16 pp., Natl. Oceanogr. Data Cent. Silver Spring, Md., 1998.

Dannenmann, S., A multi-proxy study of planktonic foraminifera to identify past millennial-scale climate variability in the East Asian Monsoon and the Western Pacific Warm Pool, Ph.D. thesis, Univ. at Albany, State University of New York, Albany, 2001.

de Garidel-Thoron, T., L. Beaufort, B. K. Linsley, and S. Dannenmann, Millennial-scale dynamics of the East Asian winter monsoon during the last 200,000 years, *Paleoceanography*, *16*, 491–502, 2001.

Dekens, P. S., D. W. Lea, D. K. Pak, and H. J. Spero, Core top calibration of Mg/Ca in tropical foraminifera: Refining paleotemperature estimation, *Geochem. Geophys. Geosyst.*, *3*(4), 1022, doi:10.1029/2001GC000200, 2002.

Douville, H., and J.-F. Royer, Sensitivity of the Asian summer monsoon to an anomalous Eurasian snow cover with the Meteo-France GCM, *Clim. Dyn.*, *12*, 449–466, 1996.

Fairbanks, R. G., M. N. Evan, J. L. Rubenstone, R. A. Mortlock, M. Moore, and C. D. Charles, Evaluating climate indices and their geochemical proxies measured incorals, *Coral Reefs*, *16*, 93–100, 1997.

Hastings, D. W., A. D. Russell, and S. R. Emerson, Foraminiferal magnesium in *Globeriginoides sacculifer* as a paleotemperature proxy, *Paleoceanography*, *13*, 150–169, 1998.

Hoerling, M. P., A. Kumar, and M. Zhong, El Niño, La Niña, and the non-linearity of their teleconnections, *J. Clim.*, *10*, 1769–1785, 1997.

Hoerling, M. P., J. W. Hurrell, and T. Xu, Tropical Origins for Recent North Atlantic Climate Change, *Science*, *292*, 90–92, 2001.

Kienast, M., S. Steinke, K. Stattegger, and S. E. Calvert, Synchronous Tropical South China Sea SST changes and Greenland warming during deglaciation, *Science*, *291*, 2132–2134, 2001.

Klein, S. A., B. J. Soden, and N. Lau, Remote sea surface variations during ENSO: Evidence for a tropical atmospheric bridge, *J. Clim.*, *12*, 917–932, 1999.

Koutavas, A., J. Lynch-Stieglitz, T. M. Marchitto, and J. P. Sachs, El Niño-like pattern in Ice Age tropical sea surface temperature, *Science*, *297*, 226–230, 2002.

Kudrass, H. R., H. Erlenkeuser, R. Vollbrecht, and W. Weiss, Global nature of the Younger Dryas cooling event inferred from oxygen isotope data from Sulu Sea cores, *Nature*, *349*, 406–409, 1991.

Kudrass, H. R., A. Hofmann, H. Doose, K. Emeis, and H. Erlenkeuser, Modulation and amplification of climatic changes in the Northern Hemisphere by the Indian summer monsoon during the past 80 k.y., *Geology*, *29*, 63–66, 2001.

Latif, M., Tropical Pacific/Atlantic Ocean inter-actions at multi-decadal time scales, *Geophys. Res. Lett.*, *28*, 539–542, 2001.

Latif, M., E. Roeckner, U. Mikolajewicz, and R. Voss, Tropical stabilization of the thermo-haline circulation in a greenhouse warming, simulation, *J. Clim.*, *13*, 1809–1813, 2000.

Lea, D. W., D. K. Pak, and H. J. Spero, Climate impact of late Quaternary Equatorial Pacific sea surface temperature variations, *Science*, *289*, 1719–1724, 2000.

Levitus, S., and T. P. Boyer, *World Ocean Atlas 1994*, vol. 4, *Temperature*, U.S. Dept. of Commerce, Washington D.C., 1994.

Linsley, B. K., Oxygen-isotope record of sea level and climate variations in the Sulu Sea over the past 15,0000 years, *Nature*, *380*, 234–237, 1996.

Linsley, B. K., and R. B. Dunbar, The late Pleistocene history of surface water $\delta^{13}C$ in the Sulu Sea: Possible relationship to Pacific deep water $\delta^{13}C$ changes, *Paleoceanography*, *9*, 317–340, 1994.

Linsley, B. K., and R. C. Thunell, The record of deglaciation in the Sulu Sea: Evidence for the Younger Dryas event in the tropical Western Pacific, *Paleoceanography*, *5*, 1025–1039, 1990.

Linsley, B. K., R. C. Thunell, C. Morgan, and D. F. Williams, Oxygen minimum expansion in the Sulu Sea, western Equatorial Pacific, during the last glacial low stand of sea level, *Mar. Micropaleontol.*, *9*, 395–418, 1985.

Martinson, D. G., N. G. Pisias, J. D. Hays, J. Imbrie, T. C. Moore, and N. H. Shackleton, Age dating and the orbital theory of the Ice Ages: Development of a high-resolution 0 to 300,000-year chronostratigraphy, *Quat. Res.*, *27*, 1–29, 1987.

Miao, Q., R. C. Thunell, and D. M. Anderson, Glacial-Holocene carbonate dissolution and sea surface temperature in the South China and Sulu seas, *Paleoceanography*, *9*, 269–290, 1994.

Nozaki, Y., D. S. Alibo, H. Amakawa, T. Gamo, and H. Hasumoto, Dissolved rare earth elements and hydrography in the Sulu Sea, *Geochim. Cosmochim. Acta*, *63*, 2171–2181, 1999.

Oppo, D. W., B. K. Linsley, Y. Rosenthal, S. Dannenmann, and L. Beaufort, Orbital and suborbital climate variability in the Sulu Sea, western tropical Pacific, *Geochem. Geophys. Geosys.*, in press, 2002.

Overpeck, J. T., D. Rind, A. Lacis, and R. Healy, Possible role of dust induced regional warming in abrupt climate change during the last glacial period, *Nature*, *384*, 447–449, 1996.

Pelejero, C., J. O. Grimalt, S. Heilig, and L. Wang, High-resolution U^{k}_{37} temperature reconstructions in the South China Sea over the past 220 kyr, *Paleoceanography*, *14*, 224–231, 1999.

Peterson, L. C., G. H. Haug, K. A. Hughen, and U. Rohl, Rapid changes in the hydrologic cycle of the tropical Atlantic during the last glacial, *Science*, *290*, 1947–1951, 2000.

Rosenthal, Y., and G. P. Lohmann, Accurate estimation of sea surface temperatures using dissolution-corrected calibrations for Mg/Ca paleothermometry, *Paleoceanography*, *17*(3), 1044, doi:10.1029/2001PA000749, 2002.

Rosenthal, Y., M. P. Field, and R. M. Sherrell, Precise determination of element/calcium ratios in calcareous samples using sector field inductively coupled plasma mass spectrometry, *Anal. Chem.*, *71*, 3248–3253, 1999.

Rosenthal, Y., G. P. Lohmann, K. C. Lohmann, and R. M. Sherrell, Incorporation and preservation of Mg in *Globigerinoides sacculifer*: Implications for reconstructing the temperature and $^{18}O/^{16}O$ of seawater, *Paleoceanography*, *15*, 135–145, 2000.

Schmittner, A., and A. C. Clement, Sensitivity of the thermohaline circulation to tropical and high latitude freshwater forcing during the last glacial-interglacial cycle, *Paleoceanography*, *17*(2), 1017, doi:10.1029/2000PA000591, 2002.

Sirocko, F., D. Leuscher, M. Staubwasser, J. Maley, and L. Heusser, High-frequency Oscillations of the Last 70,000 years in the Tropical/Subtropical and Polar Climates, in *Mechanisms of Global Climate Change at Millennial Time Scales*, *Geophys. Monogr. Ser.*, *112*, edited by P. U. Clark, R. S. Webb, and L. D. Keigwin, pp. 113–126, AGU, Washington, D. C., 1999.

Stott, L., C. Poulsen, S. Lund, and R. Thunell, Super ENSO and global climate oscillations at millennial time scales, *Science*, *297*, 222–226, 2002.

Waliser, D. E., and C. Gautier, A satellite-derived climatology of the ITCZ, *J. Clim.*, *6*, 2162–2174, 1993.

Wang, L., M. Sarnthein, H. Erlenkeuser, J. Grimalt, P. Grootes, S. Heilig, E. Ivanova, M. Kienast, C. Pelejero, and U. Plaumann, East Asian monsoon climate during the Late Pleistocene: High- resolution sediment records from the South China Sea, *Mar. Geol.*, *156*, 245–284, 1999.

Wang, Y. J., H. Cheng, R. L. Edwards, Z. S. An, J. Y. Wu, C.-C. Shen, and J. A. Dorale, A high-resolution absolute-dated late Pleistocene Monsoon record from Hulu Cave, China, *Science*, *294*, 2345–2348, 2001.

Webster, P. J., V. O. Magaña, T. N. Palmer, J. Shukla, R. A. Thomas, M. Yanai, and T. Yasunari, Monsoons: Processes, predictability, and prospects for prediction, *J. Geophys. Res*, *103*, 14,451–14,510, 1998.

Weyl, P. K., The role of the oceans in climate change: A theory of the ice ages, *Meteorol. Monogr.*, *8*, 37–62, 1968.

Wyrtki, K., Scientific results of marine investigations of the South China Sea and the Gulf of Thailand, physical oceanography of the Southeast Asian water, Univ. California, Scriptps Inst. Oceanogr., La Jolla, Calif., 1961.

Yokoyama, Y., T. M. Esat, and K. Lambeck, Coupled climate and sea-level changes deduced from Huon Peninsula coral terraces of the last ice age, *Earth Planet. Sci. Lett.*, *6017*, 1–9, 2001.

Yuan, X. J., and D. G. Martinson, Antarctic sea ice extent variability and its global connectivity, *J. Clim.*, *13*, 1697–1717, 2000.